

# A Reassessment of the ASTM Method for the Evaluation of the $J_{IC}$ Toughness

V. R. RANGANATH\*, A. N. KUMAR\*\*, R. K. PANDEY\*\*

\*National Metallurgical Laboratory, Jamshedpur-831007, India

\*\*Applied Mechanics Dept., I.I.T., New Delhi-110016 India

## ABSTRACT

A procedure has been suggested to determine the crack initiation fracture toughness parameter,  $J_{IC}$ , and the same has been compared with the ASTM E-813 method. In the course of that, the J-CTOD and the CTOD-SZW relationships have also been verified. The investigations carried out in different materials using three point bend (TPB) specimens of varying thickness suggest that the value of  $m$  in the J-CTOD relationship is different for the precrack initiation regime and the post crack initiation regime. The SZW measurements from fracture surfaces indicate a linear correlation with CTOD. A new blunting line has been proposed for the  $J_{IC}$  determination based on the observation made in the present work.

## INTRODUCTION

Several studies have projected the J-integral and the CTOD ( $\delta$ ) as the important tools of the elastic-plastic fracture mechanics (EPFM). The ASTM method [ASTM Standards, 1986] for determining  $J_{IC}$  uses a blunting line approach which is given by equation:

$$J = 2 \sigma_0 \Delta a \quad (1)$$

where  $\sigma_0$  is the flow stress. The factor 2 is obtained by taking a J-CTOD relationship of the type:

$$J = m \sigma_0 (\text{CTOD}) \quad (2)$$

where  $m$  is assumed to be equal to one. Also the crack tip stretching is understood to result in a semi circular type of deformation of the tip. The above method, although under continuous revision, of  $J_{IC}$  determination has been under much criticism [Jones *et al.*, 1984] in recent years. An attempt has been made in the present work to verify the J-CTOD and the  $\delta$ -SZW (stretched zone width) relationships for a realistic estimation of the slope of the blunting line in J-resistance curves. The effect of

thickness on the initiation toughness (particularly in the lower thickness regime) needs further investigation as literature reports conflicting trends of toughness variation with thickness [Ranganath *et al.*, 1987]. A secondary objective of the present study is to investigate the effect of thickness on the  $J_{IC}$  toughness in selected steels.

## EXPERIMENTAL

Two types of steels, a microalloyed steel (TISTEN-55) and a Ni-Cr-Mo steel (AISI 4340), have been used in the present investigation. The chemical composition and the mechanical properties of the steels are presented in Table 1. The TPB specimens were machined with crack plane normal to the rolling direction and the longitudinal axis along the rolling direction of the plate. The thickness (B) of the specimens was varied as 5, 10 and 15 mm, maintaining a constant width of 20 mm. A few specimens from AISI 4340 steel were quenched and tempered at 600°C (designated as 600T). All the specimens were provided with a fatigue crack as per ASTM standards to yield an initial crack length to width ratio (a/W) of approximately 0.5. The crack mouth opening displacement (CMOD) was measured by the standard clip gauge technique, and the load point displacement (LPD) using an LVDT. The crack growth was monitored throughout the test by employing a DC Electrical Potential Difference (EPD) method which was calibrated prior to the test. The calibration was performed both by the incremental saw cut method and by the multiple specimen heat tinting method [Ranganath, 1987a]. An excellent agreement between these two calibrations suggests that the plasticity effect is negligible on potential drop in the present investigation. By using a current density of 1 A/cm<sup>2</sup> enabled the minimum crack growth measurement of 20-30 μm. Specimens were loaded in a Tensometer at a displacement rate of 0.2 mm/min and all the above parameters were recorded at appropriate load intervals. The loading was continued until there was an appreciable load drop. After the tests the fracture surfaces of the specimens were examined under Cambridge S4-10 scanning electron microscope (SEM) with the electron beam at 45° to the fracture surface. The crack tip stretched zone was examined in particular using the SEM. A few typical fractographs showing the stretched zone are presented in Fig.1 and the stretched zone width values measured are recorded in Table 2. The detailed description of the experimental set up and calibration plots are reported elsewhere [Ranganath, 1987a].

## RESULTS AND DISCUSSION

### Evaluation of J and CTOD

In the present investigation, the J values at the original crack tip have been calculated by employing the standard relation for TPB specimens [Landes and Begley, 1974]. Besides, the J values were also calculated at the instantaneous crack tip by taking the crack growth into account [Simpson, 1980]. However, the difference between the J values at the original crack tip and that at the instantaneous crack tip was found to be not more than 7% even at the maximum crack growth measured [Ranganath, 1987a]. For calculating the CTOD, the relation given in BS 5762 [British Standards, 1979]:

$$\delta = \frac{K^2}{2E'\sigma_y} + \frac{V_p}{1 + \frac{(a+z)}{0.4(W-a)}} \quad (3)$$

was adopted.

However, for the reasons explained in the subsequent section, the CTOD values prior to the detection of crack initiation (*i.e.*, in small scale yielding regime) have been calculated by employing the following geometrical relation:

$$CTOD = \frac{V_g}{1 + \frac{(a+z)}{r(W-a)}} \quad (4)$$

where the rotational factor, r, was taken as 0.3 and the other terms have usual significance. The CTOD values, too, did not differ by more than 15% when calculated at the instantaneous and at the original crack tips.

### J-CTOD Relationship

The EPFM parameters J and CTOD are believed to be linearly related through factor m, and the flow properties of the materials, as given in equations (1 and 2). The flow stress ( $\sigma_o$ ) is usually taken as the average of the yield strength and the ultimate tensile stress of the material. Although the value of m is generally taken as 1 in the ASTM method, there exists a great deal of uncertainty about the actual value of m as well as its functional dependence on the geometrical and the material parameters [Paranjpe and Banerjee, 1979; Pratap, 1984; Shih, 1981]. In an attempt to verify the value of m, the J values have been plotted against the corresponding CTOD values in Fig.2. It may be observed from the figure that the J-CTOD plots are almost linear and their slopes are apparently independent of the specimen thickness. The m values thus obtained are presented in Fig.2. It may be noticed from Fig.2 that the m values show a distinct dependency on the material properties.

A closer examination of the J-CTOD plots reveals that the plot is not characterized by a single slope in the entire region and the initial slope of the line changes perceptibly at some point maintaining a fixed slope of line beyond that point. Interestingly when the crack initiation, as detected by EPD, CTOD ( $\delta_i$ ) (Table 2) values were superimposed on the J- $\delta$  plot, the change in slope of J-CTOD plot appeared to occur in the region of the crack initiation suggesting that the value of m is different for the pre- and the post-crack initiation regimes. It may however be noted that the use of BS 5762 method in the small scale yielding regime causes some problems vis-a-vis the J-CTOD relationship. This is because the elastic part of the CTOD is calculated as:  $K^2/2.E'\sigma_y$  in equation (3) wherein the m value (as in K-CTOD relation) is preassumed as 2. The elastic displacement being considerably large in this regime, this would affect the results significantly. This necessitated using of equation (4) with a lower value of r ( = 0.3) and a purely geometrical relationship for calculating the CTOD in small scale yielding regime. The J-  $\delta$  relationship in this regime was also found to show a linear trend and the corresponding m value was designated as  $m_p$ . A typical plot of J vs  $\delta$  in this regime is shown as in-set of Fig.2.

From the pre-crack growth  $m_p$  values and the post-crack growth  $m$  values presented in Fig.2 an important observation can be made, that is, the  $m_p$  values are significantly lower than the corresponding  $m$  values in all the cases. Also, it may be observed that both the  $m_p$  and  $m$  values increase with strain hardening component  $n$  (see Table 1). Similar observation has also been reported recently [Slatcher and Knott, 1986]. An attempt was made to compare the dependency of  $m$  (and  $m_p$ ) on the strain hardening exponent,  $n$  obtained in the present work with that given theoretically by the HRR singularity [Shih, 1981] and the results are shown in Fig.2. It may be noticed that the theoretical  $m$  values are substantially higher than the experimental  $m$  (and  $m_p$ ) values for all the cases. This disagreement between the experimental and theoretical [Shih, 1981]  $m$  values lies in the fact that the experimental values are far field CTOD, whereas the latter values are obtained at only the crack tip. However, it is interesting to note that the % difference between the theoretical and the experimental  $m$  values decreases with decreasing  $n$  values. This shows that the theoretical prediction for  $m$  can be used only for very low strain hardening materials.

#### Inter-relation Between CTOD and SZW

In order to construct a realistic blunting line for  $J$  determination from  $J$ -resistance curves, a detailed investigation of  $\sigma$ -SZW relationship along with the  $J$ -CTOD relationship is necessary. From the literature [e.g. Kolednik and Stuwe, 1987; Hopkins and Jolley, 1983], it appears that there is no consistent constant relating CTOD and SZW. The width of the stretched zone at the start of tearing is referred to as the critical stretched zone size. The crack extension starts in the mid-thickness region and spreads towards the specimen surfaces at progressively higher  $J$  or  $\sigma$  values. Hence, it may be reasoned that only the SZW measured at the mid thickness region of the fracture surface should be correlated with  $\sigma$ . A plot is made (Fig.3) between very small amounts of crack growth ( $a \leq 0.25$  mm) as measured by the EPD technique, and the corresponding CTOD values. It may be noticed that the high sensitivity of EPD technique resulted in potential changes during stretching also at the crack tip. In almost all the cases the  $\sigma$ - $\Delta a$  diagrams (Fig.3) are linear in nature in the initial part and have a tendency to deviate from linearity in the later stage. Superimposed on the figure are the SZW values obtained from measurements taken on the fractographs. The values corresponding to SZW are termed as  $\mathcal{E}$ (SZW) and presented in Table 2. As can be seen from Fig.3, in most of the cases, the SZW points lie over the linear part of the  $\sigma$ - $\Delta a$  plots. Thus, the CTOD may be approximately related to SZW as:

$$\text{CTOD} = C (\text{SZW}) \quad (5)$$

where  $C$  is the slope of the  $\sigma$ - $\Delta a$  plot. An average value of  $C$  has been taken for each of the materials and reported in Fig.3. Though the trend is not clear, it appears from the figure that the value of  $C$  is dependent on the flow properties and microstructure of the material.

#### Determination of $J_{IC}$

The ASTM method of determining  $J_{IC}$  in brief, is as follows: obtain an experimental  $J$  vs  $\Delta a$  plot, eliminate the data points lying outside the

region bounded by the offset lines of 0.15 mm and 1.5 mm drawn parallel to a blunting line ( $J = 2 \sigma_0 \Delta a$ ), then the intercept of a linear regression line drawn through the remaining data points on the blunting line is marked as  $J_c$ . If  $J_c$  satisfies the plane strain condition ( $W-a, a, B > 25 J_c / \sigma_0^2$ ), then  $J_c$  is called  $J_{IC}$ . This  $J_{IC}$  is believed to be a constant (independent of size and geometry) beyond a certain limiting specimen size. Fig.4 shows the ASTM E-813 method of obtaining  $J_{IC}$  (designated as  $J_{IC(A)}$ ) in typical experimental,  $J$  vs  $\Delta a$ , plots. The  $J_{IC(A)}$  values thus obtained for all the specimens are presented in Table 2.

In the light of the observations made in the preceding sections, the  $m$  (or  $m_p$ ) in the  $J$ - $\sigma$  relation as well as the slopes of the  $\sigma$ -SZW plots obtained earlier may be used to construct a realistic blunting line rather than depending on a too simplistic assumption with regard to the value of  $m$  ( $m = 1$ ) and a semicircular crack tip deformation during blunting. The blunting line equation may be given as:

$$J = m_p \sigma_0 (C \Delta a) \quad (6)$$

where  $m_p$  and  $C$  are defined earlier and are reported in Figs.2 and 3 respectively.

Fig.4 represents two typical experimental  $J$ - $\Delta a$  plots along with the proposed blunting lines and determining  $J_{IC}$  based on the new blunting lines. From the figure it is evident that the slopes of the ASTM blunting lines are higher than that of proposed blunting lines. The values of  $J_{IC}$  based on the experimental blunting lines are designated as  $J_{IC(e)}$  and are presented in Table 2. This table also includes the  $J_{IC}$  values obtained corresponding to the experimental stretched zone points on the respective diagrams and these are termed as  $J_{IC(SZW)}$ . It may be noted that the proposed method of evaluation of  $J_{IC}$  using the experimental blunting line, it is no more necessary to exclude the points before the 0.15 mm offset line. Nevertheless, from the experimental  $J$ - $\Delta a$  plots, it was noted that in number of cases, the points lying beyond the 1.5 mm offset line had a tendency to deviate from those lying before 1.5 mm offset line. Apparently the  $J$  dominated crack growth does not occur for higher values of  $J$ . In view of this, the linear regression line for  $J_{IC(e)}$  determination did not include points lying beyond 1.5 mm offset line. The  $J_{IC(e)}$  values were found to satisfy the plane strain requirement of  $J$  as per E-813 and may be termed as  $J_{IC}$ .

It may be observed from Table 2 that,  $J_{IC(e)}$  values in general, are less conservative than the  $J_{IC(A)}$  values and that the  $J$  values at SZW ( $J_{IC(SZW)}$ ) compare better with the  $J_{IC(e)}$  values rather than with the  $J_{IC(A)}$  values. In other words, the ASTM method appears to be more conservative and underestimates the material's crack initiation toughness. This also suggests that the blunting line equation has to be obtained in the individual cases through a knowledge of stretched zone sizes evaluated experimentally. However, the present investigation also indicated that the EPD method of monitoring the crack initiation and subsequent growth could be utilized for a fair approximation of the SZW by considering the crack growth indicated at the region where the  $\sigma$ - $\Delta a$  plot or the P-EPD plot showed a radical change in slope. In that case one does not have to turn to SEM fractography for measuring the SZW.

## Effect of Thickness on $J_{IC}$

The reports on thickness effect on  $J_{IC}$  toughness are quite controversial particularly for the subsize specimens. Keller and Munz [1979] have observed that the  $J_{IC}$  values are substantially thickness dependent in Ni-Cr-Mo steel tested in CT geometry. The same authors reported no such effect of thickness on  $J_{IC}$  in case of aluminium alloy [Berger, Keller and Munz, 1979]. Within the plane strain condition, the results of Mildner et al. [1982] and Williams [1979] showed a continuous increase in  $J_{IC}$  with specimen thickness. In a recent study by the present authors on a HSLA steel, similar inconsistencies of J variation with thickness have been observed. From the present investigation it was found that the  $J_{IC}$  ( $J_{IC(e)}$ ) toughness in TISTEN-55 decreases with increasing thickness (Table 2). It can be noted from the above table that for a three fold increase in thickness from 5 mm to 15 mm in TISTEN-55, the toughness decreases by 15%. The same change in thickness in AISI 4340 steel tested in as-received condition brought an increase of toughness from 27 to 75 kJ/m<sup>2</sup>. However, for the 600T condition no specific trend of toughness variation with thickness was noted. As can be gathered from literature, such types of variations are not uncommon. Further investigation is required to ascertain the thickness dependence of  $J_{IC}$  toughness in materials of different yield strengths particularly in the subsize specimens.

## CONCLUSIONS

1. A new equation for blunting line is proposed for the evaluation of  $J_{IC}$  toughness. The  $J_{IC}$  values obtained by this method are in good agreement with  $J_{IC(SZW)}$  values and are generally less conservative than the values obtained by ASTM E-813 method.
2. The J- $\delta$  relationship may be expressed by  $\delta = J/m \sigma_0$  where the value of m in the pre-crack initiation regime (designated as  $m_p$ ) is found to be smaller than that in the post crack initiation regime (m). The m values appear to be independent of thickness, however, the strain hardening exponent of the material appears to influence the value of m.
3. Crack tip stretch zone is related to the CTOD as:  $\delta = C(SZW)$ , where C is numerical factor and it appears to depend on the flow properties. The EPD technique may provide a fair estimation of SZW from the P vs EPD (or  $\delta$  vs  $\Delta a$ ) plots.
4. The J-R curves developed by EPD technique show two distinct slopes, the initial slope indicating the notional separation of material at the crack tip (due to stretching) and the latter due to stable tearing.
5. The thickness dependence of  $J_{IC}$  appears to be a function of the material flow properties, however, thickness dependence of fracture toughness does not reveal a consistent trend.

## REFERENCES

- ASTM Standards, Vol.0301 (1986), E-813, pp.762-780.  
 Berger, C., H.P.Keller and D.Munz (1979), ASTM STP 668, p.378.  
 British Standards: 5762, 1979.

- Hopkins, P. and G.Jolley (1983), Engng.Fract.Mech., 18, p.239.  
 Jones, R.L. et al. (1984), Procs. of Int. Conf. on Fract. (ICF-6), Vol.5, p.3409.  
 Keller, H.P. and D.Munz (1979), ASTM STP 631, p.378.  
 Kolednik, O. and H.P.Stuwe (1987), Int.Jl.Fract., 33, R-63.  
 Landes, J.D. and J.A.Begley (1974), ASTM STP 460, p.170.  
 Mildner, H. et al. (1982), Fracture and Fracture Toughness, Vol.1, Cradley Heath Warely, U.K., p.207.  
 Paranjpe, S.A. and S.Banerjee (1979), Engng.Fract.Mech., 11, p.43.  
 Pratap, C.R. (1984), Ph.D. Thesis, I.I.T., Delhi.  
 Ranganath, V.R., A.N.Kumar and R.K.Pandey (1987), Proc. of Conf. on Mech. Behavior of Materials (ICMB-5), Paper No.1-23.  
 Ranganath, V.R. (1987a), Ph.D. Thesis, I.I.T., Delhi.  
 Shih, C.F. (1981), Jl. of Mech. Phys. & Sol., 29, p.305.  
 Simpson, L.A. (1980), Int. J. of Fract., 16, R-247.  
 Slatcher, S. and J.F.Knott (1986), Matl. Sc. and Engng., 82, p.37.  
 Williams, J.A. (1979), Report No. RUREG/CR-9859, HED Lab., Richland, p.48.

Table 1(A): Chemical Composition (wt.%)

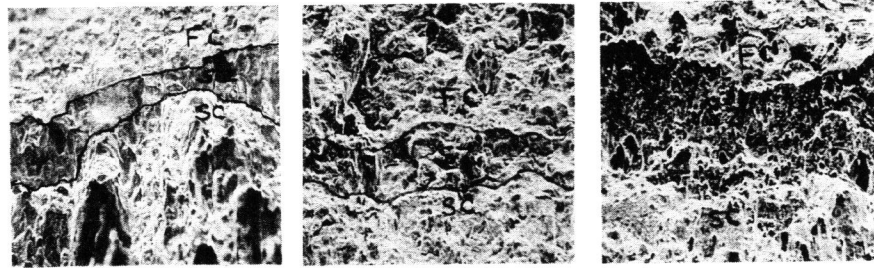
Material	C	Mn	Si	P	S	V	Ni	Cr	Mo
TISTEN-55	0.18	1.44	0.25	0.025	0.024	0.07	-	-	-
AISI 4340	0.39	0.53	0.23	0.26	0.015	-	1.49	0.97	0.21

Table 1(B): Mechanical Properties

Material/condition	$\sigma_y$ , MPa	$\sigma_u$ , MPa	% El	% RA	n
TISTEN-55	413	569	31	74	0.220
AISI 4340 (A.R)	393	740	17	52	0.256
AISI 4340 (600T)	1197	1236	13	57	0.029

Table 2: Thickness Dependence of SZW, CTOD and J Toughness Values

Material	B	SZW	$\delta_l$	$\delta_{SZW}$	$J_{IC(SZW)}$	$J_{IC(A)}$	$J_{IC(e)}$
	mm	$\mu m$	$\mu m$	m	kJ/m <sup>2</sup>	kJ/m <sup>2</sup>	kJ/m <sup>2</sup>
TISTEN-55	5	178	37	71	65	50	77
	10	110	25	58	51	44	57
	15	185	16	57	55	41	66
AISI 4340 (A.R)	5	97	33	43	31	28	27
	10	120	32	47	47	34	32
	15	84	56	71	78	92	75
AISI 4340 (600T)	5	109	16	23	35	27	33
	10	83	37	45	63	59	62
	15	95	11	17	19	14	19



(a) TISTEN-55, B=5mm, 140X (b) 4340(A.R), B=15mm, 185X (c) 600T, B=10mm, 250X

FC: Fatigue Crack; SZ: Stretched Zone; SC: Stable Crack Growth.

Fig.1 Typical Fractographs Showing SZW

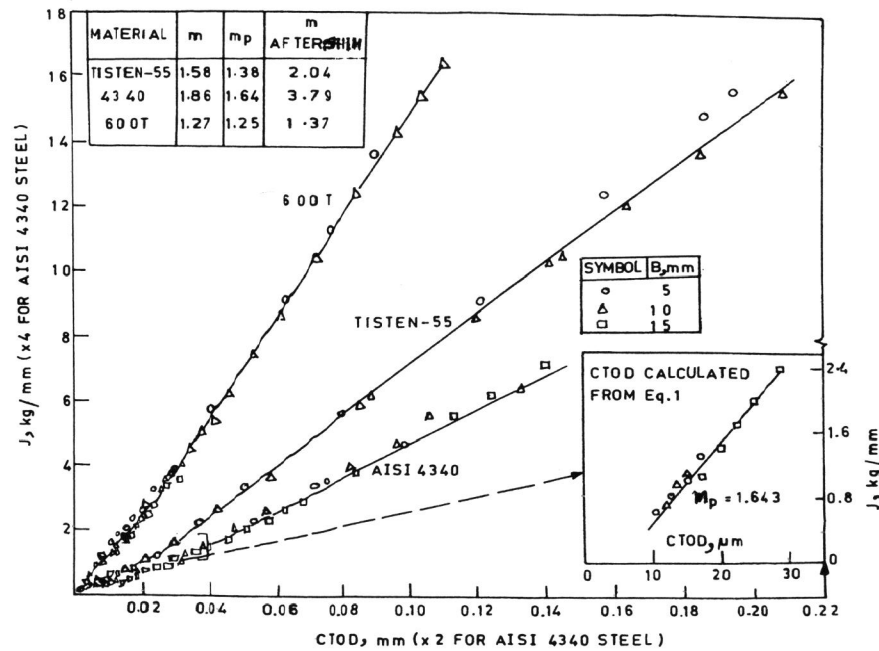


FIG.2 J-CTOD RELATIONSHIP IN TPB SPECIMENS OF MATERIALS UNDER INVESTIGATION

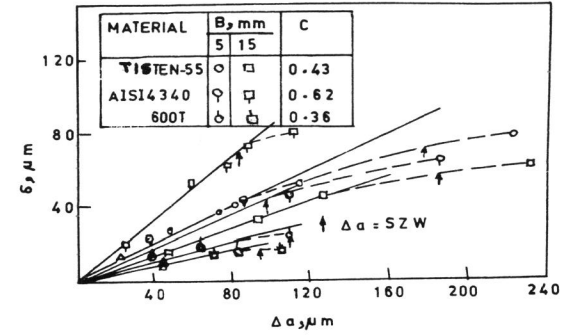


FIG.3 INITIAL PART OF  $\delta - \Delta a$  RELATIONSHIP

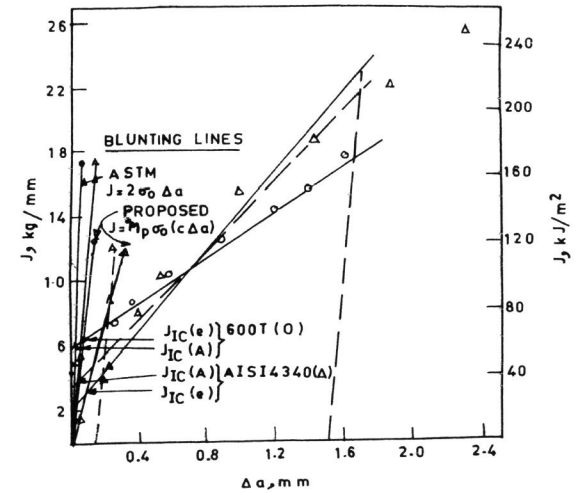


FIG.4 DETERMINATION OF  $J_{IC}$  BY THE PROPOSED METHOD